Electronic Supplementary Material (ESI) for New Journal of Chemistry

A Cd-based perovskite with optical-electrical multifunctional response

Li-Jun Han,[a] Jia Liu,[a] Ting Shao,[a] Qiang-Qiang Jia,[a] Chang-Yuan Su,[b] Da-Wei Fu*[a], Hai-Feng Lu*[a]

[a] Institute for Science and Applications of Molecular Ferroelectrics, Key Laboratory of the Ministry of Education for Advanced Catalysis Materials, Zhejiang Normal University, Jinhua, 321004, People's Republic of China.

[b] Ordered Matter Science Research Center, Jiangsu Key Laboratory for Science and Applications of Molecular Ferroelectrics, Southeast University, Nanjing 211189, People's Republic of China.

Table of contents

Experimental measurement methods

Single crystal synthesis

The 2D organic-inorganic hybrid perovskite, $(TMA)_2CdCl_4$, could be obtained easily. A certain stoichiometric amount of thiophene-2-methylamine (4 mmol) and cadmium chloride (2 mmol) were mixed in ethanol solvent at a 2:1 molar ratio, followed by the addition of excess concentrated hydrochloric acid to make the solution clarified, then filtered into a clean beaker. The mixed solution was slowly evaporated under room temperature to attain the product as colorless transparent crystal. All analytical grade reagents and solvents required for experiment were purchased directly and used without further purification. It should be noted that the ratio of thiophene-2-methylamine to cadmium chloride should not be less than 2:1, and the amount of hydrochloric acid should not exceed four times that of amine. The solvent is 75% ethanol, otherwise it will be difficult to prepare crystals with better quality. These experimental parameters are the key to guaranteeing the reproducibility of as-prepared crystals.

Physical measurements

The single-crystal X-ray diffraction (XRD), powder XRD, differential scanning calorimetry (DSC) measurements, dielectric measurements, Hirshfeld surface analysis, thermogravimetric analysis (TGA), absorption and photoluminescence spectra were profiled one by one. The details of the characterization method of the instrument are as follows.

Thermal measurements

DSC measurement is used to verify the thermal anomaly of the compound during heating and cooling. After several experimental measurements, it was found that the compound undergoes a phase transition. DSC measurement of $(TMA)_2CdCl_4$ was carried out by PerkinElmer Diamond DSC instrument in a nitrogen atmosphere, 12 mg powder samples of compound were weighed and placed in an aluminum crucible, the heating and cooling cycles were then carried out in the temperature range from 370 K to 430 K at a rate of 20 K min^{-1}.

Thermogravimetric analysis (TGA) was performed on a TA Q50 system in the temperature range of 300 K to 1050 K at a heating rate of 10 K min^{-1}. The thermal stability of the compound can be measured by TGA.

Single-crystal X-ray diffraction

The structural phase transition of the crystal is caused by the change of symmetry. Generally, the structural symmetry inside the crystal at HTP is higher than that at LTP. Structural changes were analyzed by measuring the crystal structure before and after the phase transition. It should be noted that we select a single crystal with a size of $0.25\times0.25\times0.25$ mm^3 with better quality under the microscope to obtain a better data. Variable-temperature single-crystal XRD data of the compound was collected by using Bruker APEX-II CCD with Mo Kα radiation (λ = 0.71073 Å) at 300 K and 430 K. Date processing was finished by the APEX-III. Variable-temperature crystal

structures were solved using a direct method and subsequent continuous Fourier synthesis. Subsequently, these crystals were refined by full-matrix leastsquares methods based on F2 using the SHELXTL software package. Eventually, in addition to the basic structure and packing diagrams of the compound were drawn by DIAMOND software, other relevant crystallographic data and structure refinement at 300 K and 430 K are listed in Table S1 in supporting information.

Powder X-ray diffraction

Powder X-ray diffraction (PXRD) data for the compounds were measured using a Bruker D8 Advance X-ray diffraction system with Cu-Kα radiation in the 2θ range of 5°-55° with a step size of 0.02°.

Hirshfeld surfaces analysis

Hirshfeld surfaces and the related 2D-fingerprint plots were calculated by using the CrystalExplorer program with inputting structure file in CIF format. In this work, all the Hirshfeld surfaces were generated using a standard (high) surface resolution. The 3D Hirshfeld surfaces and 2D fingerprint plots are unique for any crystal structure. The intensity of molecular interaction is mapped onto the Hirshfeld surface by using the respective red-blue-white scheme: where the white or green regions exactly correspond to the distance of Van der Waals contact, the blue regions correspond to longer contacts and the red regions represent closer contacts. In 2D fingerprint plots, each point represents an individual pair (d_i, d_e), reflecting the distances to the nearest atom inside (d_i) and outside (d_e) of the Hirshfeld d_{norm} surface.

The normalized contact distance d_{norm} is based on d_e, d_i and the van der Waals (vdW) radii of the two atoms external (r_e^{vdW}) and internal (r_i^{vdW}) to the surface:

$$d_{\text{norm}} = \frac{d_i - r^{vdW}}{r_i^{vdW}} + \frac{d_e - r}{r_e^{vdW}}$$

d_{norm} surface is used for the identification of close intermolecular interactions.
Hirshfeld defined a weight function for each atom in a molecule, by this we mean that all hydrogen atoms need to be located accurately, as do the location and identity of solvent molecules, and any disorder present needs to be modelled and information about disorder groups included in the CIF file. Furthermore, in order to make meaningful comparisons between crystal structures it is essential that bond distances to H atoms are standardised to realistic values. For this purpose, CrystalExplorer uses average bond distances derived from neutron diffraction experiments.

Dielectric Measurements

For the structural phase transition, it will be obvious that dielectric anomalies emerge near the phase transition temperature. Dielectric measurement is an important means to detect whether the substance has undergone a phase transition. The crystal powder was pressed into a tablet, followed by being coated with carbon glue and attached to copper wires. It should be noted that the area of the adhesive sheet should be 2×2 mm^2, and the thickness should be <1 mm, so that the measured error will be less than 2%. Complex dielectric constants measurement in the heating and cooling cycles were performed on Tonghui TH2828A instrument over the frequency range of 500 Hz to 1 MHz. The compressed tablet and single-crystal sample of the compound was

deposited with silver conducting glue, it is then used as an electrode for dielectric measurement.

Photoluminescence measurements

The absorption spectra of $(TMA)_2CdCl_4$ microscale crystals were recorded on a PE Lambda 900 UV-Vis-NIR spectrum photometer at ambient temperature with $BaSO_4$ used as the standard reference. At the edge wavelength of the working band of the UV-Vis spectrophotometer, due to the low transmittance of the monochromator, the radiation intensity of the light source, and the sensitivity of the detector, the influence of stray light is more significant. This is a major source of experimental error in spectral measurements. In the measurement process, the filter or filter solution is mainly used to test the stray light of the UV-Vis spectrophotometer.

Photoluminescence measurements were performed on an Edinburgh FLS980 fluorescence spectrometer. During the measurement process, we reduce the experimental error by controlling the uniformity of the sample, handling the interference of spectral lines (by placing a filter between the analysis crystal and the detector), and regulating the instruments and equipment strictly. The colorimetric coordinate computing software was used to calculate the CIE coordinates, correlated color temperature (CCT) and CRI.

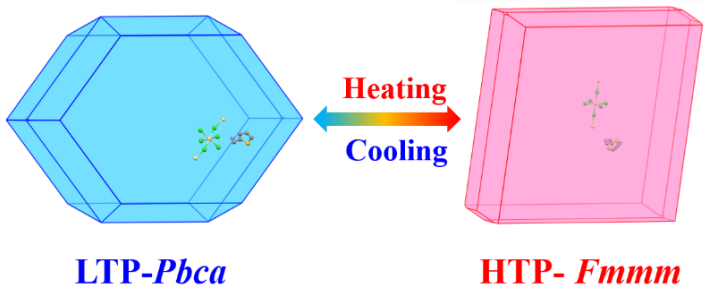

Figure S1. Simulated single crystal diagrams at 300 K and 430 K of the compound.

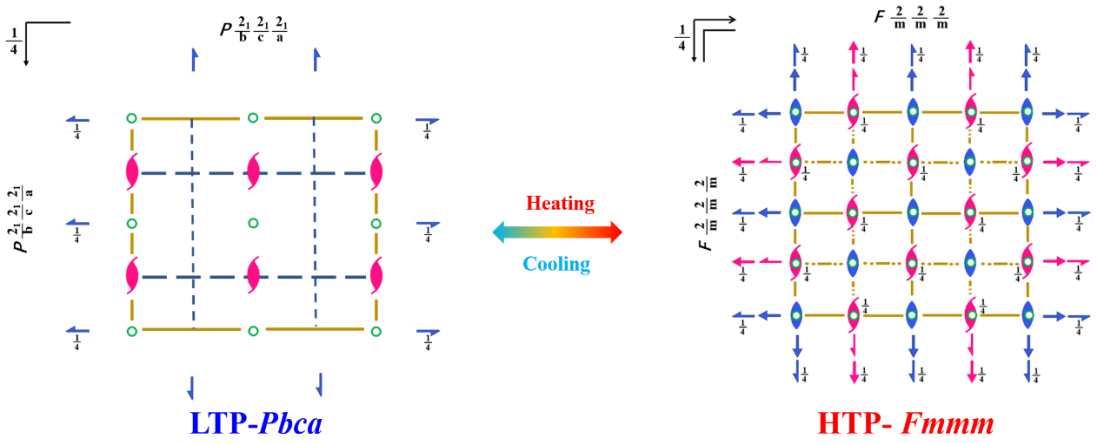

Figure S2. Symmetric change of the compound from the LTP (*Pbca*) to the HTP (*Fmmm*).

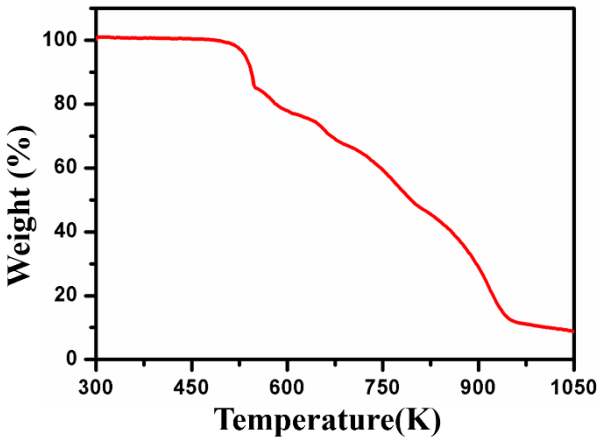

Figure S3. TGA curve of $(TMA)_2CdCl_4$ in the temperature range of 300 K-1050 K.

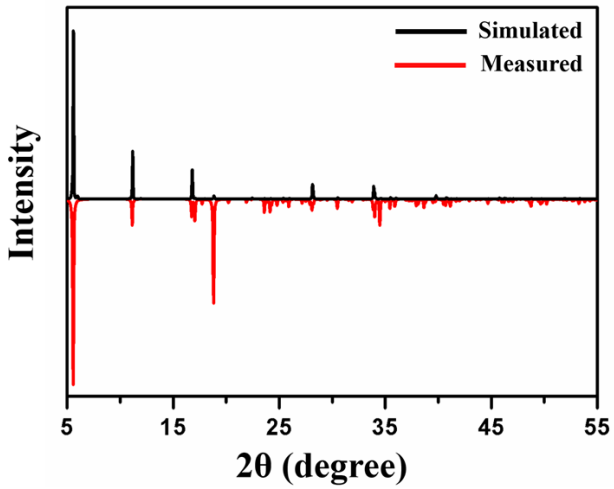

Figure S4. Measured and simulated powder X-ray diffraction patterns of $(TMA)_2CdCl_4$ at 298 K.

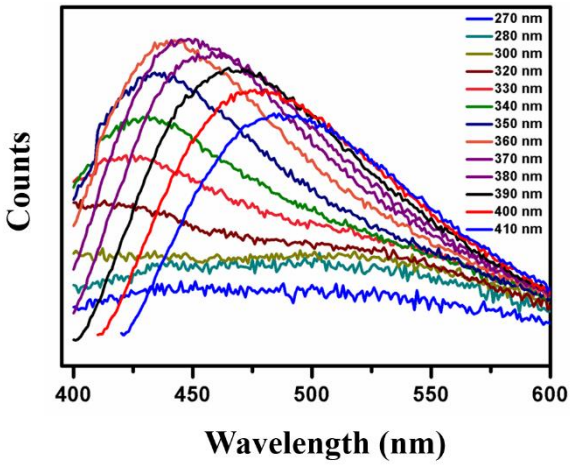

Figure S5. Fluorescence emission spectra measured with different excitation wavelengths.

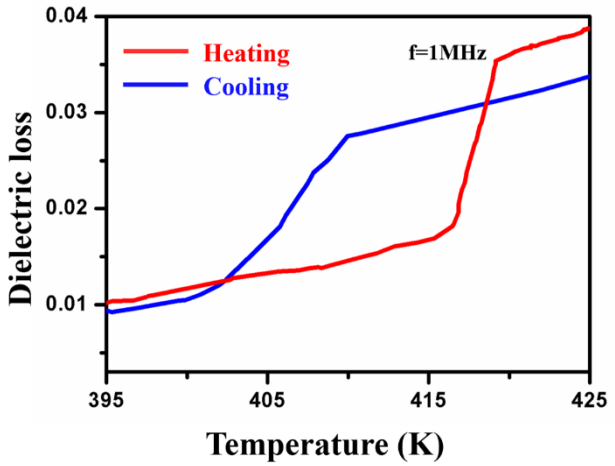

Figure S6. Dielectric loss (tan δ) of the compound at 1 MHz in the heating-cooling run.

Table S1. Phase transition temperature (T_r) comparison of reported two-dimensional cadmium-based perovskites

Compound	T_r/K	Reference
$(TMA)_2CdCl_4$	420.9	This work
$(CH_3NH_3)_2CdCl_4$	283	[1]
MA_2CdI_4	173/283	[2]
$[(CH_3)_2NH_2][Cd(N_3)_3]$	175	[3]
$[C_6H_5(CH_2)_4NH_3]_2CdCl_4$	304/338	[4]
$[(C_3H_7)_4N][Cd(N(CN)_2)_3]$	245	[5]
[3-3difluorocyclobutylammonium]$_2CdCl_4$	353.9	[6]
$[NH_3(CH_2)_5NH_3]CdCl_4$	337/417	[7]
[(*R*)-β-MPA]$_2CdCl_4$	343	[8]
[(*S*)-β-MPA]$_2CdCl_4$	343	[8]
$[(CH_2)_{12}(NH_3)_2]CdCl_4$	376.8	[9]

Table S2. Crystal data and structure refinements of $(TMA)_2CdCl_4$ at 300 K and 430 K.

Compound	**LTP** (300 K)	**HTP** (430 K)
Empirical formula	$C_{10}H_{16}CdCl_4N_2S_2$	$C_{10}H_{16}CdCl_4N_2S_2$
Formula weight	482.57	482.57
Crystal system	Orthorhombic	Orthorhombic
Space group	*Pbca*	*Fmmm*
a (Å)	7.5349 (7)	7.459(4)
b (Å)	7.3677 (7)	7.598(3)
c (Å)	31.746 (3)	31.724(13)
α (°)	90	90
β (°)	90	90
γ (°)	90	90
Volume (Å^3)	1762.4 (3)	1797.8(14)
Z	4	4
Radiation type	Mo-Ka	Mo-Ka
Absorption correction	Multi-scan	Multi-scan
F (000)	952	952
GOF	1.18	1.02
R_1	0.069	0.138
wR_2	0.269	0.347

Table S3. Selected bond lengths [Å] and bond angles [°] for $(TMA)_2CdCl_4$ at 300 K.

Temperature	Bond lengths [Å]		Bond angles [°]	
300 K	Cd1—Cl3^{i}	2.561 (2)	Cl3^{i}—Cd1—Cl3	180.0
	Cd1—Cl3	2.561 (2)	Cl3^{i}—Cd1—Cl1^{ii}	90.86 (8)
	Cd1—Cl1^{ii}	2.663 (2)	Cl3—Cd1—Cl1^{ii}	89.14 (8)
	Cd1—Cl1^{iii}	2.663 (2)	Cl3^{i}—Cd1—Cl1^{iii}	89.14 (8)
	Cd1—Cl1	2.686 (2)	Cl3—Cd1—Cl1^{iii}	90.86 (8)
	Cd1—Cl1^{i}	2.686 (2)	Cl1^{ii}—Cd1—Cl1^{iii}	180.0
	Cl1—Cd1^{iv}	2.663 (2)	Cl3^{i}—Cd1—Cl1	88.52 (7)
	S4—C1	1.682 (16)	Cl3—Cd1—Cl1	91.48 (7)
	S4—C4	1.719 (12)	Cl1^{ii}—Cd1—Cl1^{i}	87.863 (17)
	C4—C3	1.439 (15)	Cl1^{iii}—Cd1—Cl1^{i}	92.136 (18)
	C4—C5	1.468 (18)	Cl3^{i}—Cd1—Cl1	91.48 (7)
	C3—C2	1.416 (17)	Cl3—Cd1—Cl1	88.52 (7)
	C3—H3	0.9300	Cl1^{ii}—Cd1—Cl1	92.137 (18)
	C5—N2	1.510 (13)	Cl1^{iii}—Cd1—Cl1	87.864 (18)
	C5—H5A	0.9700	Cl1—Cd1—Cl1^{i}	180.0
	C5—H5B	0.9700	Cd1^{iv}—Cl1—Cd1	160.26 (11)
	C2—C1	1.33 (2)	C1—S4—C4	92.1 (8)
	C2—H2	0.9300	C3—C4—C5	126.3 (11)
	C1—H1	0.9300	C3—C4—S4	111.4 (10)
	N2—H2A	0.8900	C5—C4—S4	122.2 (9)
	N2—H2B	0.8900	C2—C3—C4	107.7 (12)
	N2—H2C	0.8900	C2—C3—H3	126.1
			C4—C3—H3	126.1
			C4—C5—H5A	109.0
			C4—C5—H5B	109.0
			N2—C5—H5B	109.0
			H5A—C5—H5B	107.8
			C1—C2—C3	116.2 (14)
			C1—C2—H2	121.9
			C3—C2—H2	121.9
			C2—C1—S4	112.5 (11)
			C2—C1—H1	123.7
			S4—C1—H1	123.7
			C5—N2—H2A	109.5
			C5—N2—H2B	109.5
			H2A—N2—H2B	109.5
			C5—N2—H2C	109.5
			H2A—N2—H2C	109.5
			H2B—N2—H2C	109.5

Symmetry codes: (i) −x+1, −y, −z+1; (ii) x+1/2, −y+1/2, −z+1; (iii) −x+1/2, y−1/2, z; (iv) x−1/2, −y+1/2, −z+1.

Table S4. Selected bond lengths [Å] and bond angles [°] for $(TMA)_2CdCl_4$ at 430 K.

Temperature	Bond lengths [Å]		Bond angles [°]	
430 K	N1—C1	1.5199 (6)	C1—N1—C1^{i}	44.45 (2)
	N1—C1^{i}	1.5199 (6)	C2—C1—N1^{i}	135.23 (2)
	C1—C2	1.4998 (6)	C2—C1—N1^{iii}	135.23 (2)
	C2—C5^{ii}	1.5004 (6)	C2—C1—N1	135.23 (2)
	C2—C5^{i}	1.5004 (6)	C2—C1—N1^{ii}	135.23 (2)
	C2—C5	1.5004 (6)	C1^{ii}—C2—C1^{i}	45.08 (3)
	C2—S1	1.6753 (6)	C1^{i}—C2—C1	45.08 (3)
	C2—S1^{ii}	1.6753 (6)	C1^{ii}—C2—C1^{iii}	45.08 (3)
	C2—S1^{i}	1.6753 (6)	C1^{i}—C2—C1^{iii}	45.08 (3)
	Cd1—Cl1^{iv}	2.499(8)	C1^{ii}—C2—C5^{ii}	143.678(18)
	Cd1—Cl1	2.499(8)	C1^{i}—C2—C5^{ii}	143.678(18)
	Cd1—Cl2^{v}	2.6618 (9)	C1—C2—C5^{ii}	98.59 (3)
	Cd1—Cl2^{vi}	2.6618 (9)	C1^{iii}—C2—C5^{ii}	98.59 (3)
	Cd1—Cl2	2.6618 (9)	C1^{i}—C2—C5^{i}	143.678(18)
	Cl2—Cd1^{vii}	2.6618 (9)	C1^{ii}—C2—C5^{i}	143.678(18)
	S1—C3^{iii}	1.5491 (7)	C1—C2—C5^{i}	98.59 (3)
	S1—C3	1.5491 (7)	C1^{iii}—C2—C5^{i}	98.59 (3)
	C4—C5	1.5002 (8)	C1—C2—C5	143.678(18)
	C4—C3	1.5004 (9)	C1^{iii}—C2—C5	143.678(18)
	C3—C5^{ii}	1.8822 (8)	Cl1—Cd1—Cl1^{iv}	180.0
	C3—C5^{i}	1.8822 (8)	Cl1—Cd1—Cl2^{v}	90.0
	N1—H1A	0.8901	Cl1^{iv}—Cd1—Cl2^{v}	90.0
	N1—H1B	0.8900	Cl1^{iv}—Cd1—Cl2^{vi}	90.0
	N1—H1C	0.8900	Cl1^{iv}—Cd1—Cl2^{vi}	90.0
	C1—H1D	0.9700	Cl2^{v}—Cd1—Cl2^{vi}	180.0
	C1—H1E	0.9700	Cl1—Cd1—Cl2	90.0
	S1—H3	1.5883	Cl1^{iv}—Cd1—Cl2	90.0
	S1—H5^{ii}	1.5883	Cl2^{v}—Cd1—Cl2	91.06 (4)
	C4—H4	0.9300	Cl2^{vi}—Cd1—Cl2	88.94 (4)
	C4—H3^{i}	0.4887	Cl1—Cd1—Cl2^{vii}	90.0
	C4—H4^{viii}	1.1679	Cl1^{iv}—Cd1—Cl2^{vii}	90.0
	C3—H3	0.9449	Cl2^{v}—Cd1—Cl2^{vii}	88.94 (4)
	C5—H5	0.9296	Cl2^{vi}—Cd1—Cl2^{vii}	91.06 (4)
			Cl2—Cd1—Cl2^{vii}	180.0
			Cd1^{ix}—Cl2—Cd1	180.0
			C3^{iii}—S1—C2	99.35 (4)
			C3—S1—C2	99.35 (4)
			S1^{ii}—C4—C3	102.69 (3)
			S1^{i}—C4—C3	102.69 (3)
			C5—C4—C3	103.08 (3)
			C4^{ii}—C3—C4	160.94 (8)
			C4^{i}—C3—C4	160.94 (8)

C4^{ii}—C3—S1	43.98 (5)
C4^{i}—C3—S1	43.98 (5)
C4—C3—S1	116.95 (4)
C4^{ii}—C3—C5^{ii}	48.67 (5)
C4^{i}—C3—C5^{ii}	48.67 (5)
C4—C3—C5^{ii}	112.27 (4)
S1—C3—C5	4.682 (3)
C4^{ii}—C3—S1^{i}	128.53 (6)
C4^{i}—C3—S1^{i}	128.53 (6)
C4—C3—S1^{i}	32.41 (2)
S1^{ii}—C5—C4	1.235 (15)
S1^{i}—C5—C4	1.235 (15)
S1^{ii}—C5—C2	113.09 (2)
S1^{i}—C5—C2	113.09 (2)
C4—C5—C2	114.33 (3)

Symmetry codes: (i) −x+2, −y+2, z; (ii) x, −y+2, z; (iii) −x+2, y, z; (iv) −x, −y+1, −z; (v) −x+1/2, y+1/2, −z; (vi) −x, y, −z; (vii) x−1/2, y+1/2, z; (viii) x, −y+3/2, −z+1/2; (ix) x+1/2, y−1/2, z.

Table S5. Bond lengths and bond angles of hydrogen bonding at 300 K.

D—H···*A*	*D*—H[Å]	H···*A*[Å]	*D*···*A*[Å]	*D*—H···*A*[Å]
N2—H2C···Cl3^{v}	0.89	2.40	3.288 (9)	173
N2—H2B···Cl1^{ii}	0.89	2.52	3.291 (10)	145
N2—H2B···Cl1^{v}	0.89	2.99	3.477 (8)	117
N2—H2A···Cl3^{iv}	0.89	2.36	3.223 (8)	163
C5—H5B···Cl3^{ii}	0.97	2.77	3.692 (12)	158
C5—H5A···Cl3^{i}	0.97	2.82	3.736 (12)	158

Symmetry codes: (i) −x+1, −y, −z+1; (ii) x+1/2, −y+1/2, −z+1; (iv) x−1/2, −y+1/2, −z+1; (v) −x+1, −y+1, −z+1.

Table S6. Bond lengths and bond angles of hydrogen bonding at 430 K.

D—H···*A*	*D*—H[Å]	H···*A*[Å]	*D*···*A*[Å]	*D*—H···*A*[Å]
N1—H1A···Cl2^{x}	0.89	2.75	3.447 (10)	136
N1—H1A···Cl2^{vii}	0.89	2.75	3.447 (10)	136
N1—H1B···Cl2^{ix}	0.89	2.75	3.447 (10)	136
N1—H1C···Cl2 ^{viii}	0.89	2.75	3.447 (10)	136

Symmetry codes: (vii) −x+1, y+1, −z; (viii) x+1/2, y+1/2, z; (ix) −x+3/2, y+1/2, −z; (x) x+1, y+1, z.

Table S7. H_{inside}-$Cl_{outside}$ surface area, mean d_i, mean d_e and mean d_{norm} of different cations in the compound.

Temperature	Hinside-Cloutside surface area (%)	mean d_i	mean d_e	mean d_{norm}
300K	0.283	1.68	1.88	0.45
430K	0.271	1.59	1.80	0.38

Reference

1. A. Ran Lim, S. Wan Kim and Y. Lak Joo, *J. Appl. Phys.*, 2017, **121**, 215501.
2. R. Roccanova, W. Ming, V. R. Whiteside, M. A. McGuire, I. R. Sellers, M.-H. Du and B. Saparov, *Inorg. Chem.*, 2017, **56**, 13878-13888.
3. M. Trzebiatowska, M. Maczka, M. Ptak, L. Giriunas, S. Balciunas, M. Simenas, D. Klose and J. Banys, *J. Phys. Chem. C*, 2019, **123**, 11840-11849.
4. L. Sui Li, W. Juan Wei, H. Qiang Gao, Y. Hui Tan and X. Bo Han, *Chem.Eur. J*, 2021, **27**, 9054-9059.
5. M. Maczka, A. Gagor, M. Ptak, D. Stefanska and A. Sieradzki, *Phys. Chem. Chem. Phys.*, 2018, **20**, 29951-29958.
6. T. Shao, J. M. Gong, J. Liu, L. J. Han, M. Chen, Q. Jia, D. W. Fu and H.-F. Lu, *Chem. Eng. Commun.*, 2022, **24**, 4346.
7. A. R. Lim and Y. L. Joo, *Sci. Rep.*, 2022, **12**. 4251.
8. Y.-K. Li, T.-T. Ying, H. Zhang, Y.-H. Tan, Y.-Z. Tang, F.-X. Wang and M.-Y. Wan, *Dalton Trans.*, 2022, **51**, 6860-6867.
9. M. F. Mostafa and A. Hassen, *Phase Transitions*, 2006, **79**, 305-321.